universität wien

MASTERARBEIT / MASTER'S THESIS

Titel der Masterarbeit / Title of the Master's Thesis

„Cytoarchitectonic mapping and high-resolution 3D-reconstruction of the bed nucleus of stria terminalis in the human brain“

verfasst von / submitted by

Andrea Brandstetter, BSc

angestrebter akademischer Grad / in partial fulfilment of the requirements for the degree of

Master of Science (MSc)

Wien, 2017 / Vienna 2017

Studienkennzahl lt. Studienblatt / degree programme code as it appears on the student record sheet:	A 066 831
Studienrichtung lt. Studienblatt / degree programme as it appears on the student record sheet:	Masterstudium Zoologie
Betreut von / Supervisor:	Prof. Dr. med. Katrin Amunts

Declaration of Authorship

I confirm that this Master's thesis is my own work and I have documented all sources and material used.

This thesis was not previously presented to another examination board and has not been published.

Place and date

Signature

This thesis was realized in collaboration with Forschungszentrum Jülich GmbH at the Institute of Neuroscience and Medicine, Structural and functional organisation of the brain (INM-1).

Acknowledgements

First of all, I would like to thank my supervisor **Prof. Dr. med. Katrin Amunts** for her continuous support and encouragement during my thesis at INM-1. I appreciate our fruitful discussions as her teaching me to work independently and take own decisions.

I was also supported by my mentor **Prof. Dr. Thomas Hummel**, university of Vienna. He remained interested and curious about my topic when I presented my preliminary results in Vienna, even if it was not directly related to his own research activities.

I would like to thank **Hartmut Mohlberg** for his excellent accomplishments with probability maps and 3D-reconstructions, but also for his helpful technical information on image processing.

I am particularly grateful to **Sebastian Bludau**, **Olga Kedo** and **Daniel Zachlod** for their guidance. They were always willing to discuss questions and challenges I faced during cytoarchitectonic mapping and gave me important feedback while writing this thesis.

Special thanks goes to **Prof. Dr. med. Karl Zilles** for sharing images and profound knowledge of receptorautoradiography as well as **Dipl.-Phys. David Gräßel** for providing data and insights of Polarized Light Imaging technique.

I sincerely appreciate the cooperation and explanations of **Sarah Haas** and **Marcel Huysegoms** of the Big Data Analytics group in image registration. In particular, I would also like to thank Marcel Huysegoms for his excellent introduction to LaTeX, other IT-supports and his honest remarks while writing this thesis.

For their technical support and providing histological or digitized images I would like to thank René Hübbers, Janshan Rajenthiran and Jessica Teske-Bausch of INM-1.

I would like to thank the following people for proofreading this thesis or parts of it, or for their contribution to technical and organizational matters: Haimasree Bhattacharya, Johanna Brandstetter, Mira Großschmidt, Nora Großschmidt, Marlene Karelly, Julia Scheuvens, Georg Semanek, Hannah Spitzer, Maria Wieser and Maria-Christine Zaniat.

Finally, I would like to express my appreciation to my family and friends who supported my decision when I moved to Germany and gave me advice whenever I needed.

Contents

Abstract

The bed nucleus of the stria terminalis, a subcortical gray matter structure of the basal forebrain, is involved in fear response and stress situations. In the present study the bed nucleus was cytoarchitectonically mapped on histological sections of ten human postmortem brains. Distinct criteria were applied, such as size, shape or distribution of neurons, giving each region of the brain a particular cytoarchitectonic pattern. Four subdivisions within the lateral and medial subnuclei of the bed nucleus of the stria terminalis were identified. These subdivisions are herein presented in a high-resolution 3D-reconstruction, which provides detailed information about the specific shape of each of the subdivisions of the bed nucleus. Individual delineations in the ten brains were the basis for probabilistic maps in stereotactic space. These maps demonstrate the interindividual variability of both subnuclei (lateral and medial). In addition, the borders of the subdivisions were examined also by alternative modalities, such as quantitative receptorautoradiography and 3D-Polarized Light Imaging.

Zusammenfassung

Der bed nucleus der stria terminalis, ein subkortikales Kerngebiet im basalen Vorderhirn, ist in Angstreaktionen oder Stresssituationen involviert. In dieser Arbeit wurde der bed nucleus auf histologischen Schnitten in zehn menschlichen postmortem Gehirnen kartiert. Bestimmte Kriterien wie Größe, Form oder Verteilung der Neurone wurden angewandt, um Regionen anhand ihrer zytoarchitektonischen Muster voneinander zu unterscheiden. Vier Unterteilungen innerhalb des lateralen und medialen Unterkerns des bed nucleus der stria terminalis konnten gefunden werden. Diese Unterteilungen werden in dieser Arbeit mittels hoch-aufgelöster 3D-Rekonstruktion präsentiert, um detaillierte Information über die spezifische Form eines jeden Gebietes des bed nucleus zu erhalten. Die individuellen Abgrenzungen in allen zehn Gehirnen waren die Grundlage für Wahrscheinlichkeitskarten im stereotaktischen Raum. Diese Karten stellen die interindividuelle Variabilität beider Unterkerne (lateral und medial) dar. Außerdem wurden die Ergebnisse stichprobenartig mit alternativen Modalitäten, der quantitativen Rezeptorautoradiographie und 3D-Polarized Light Imaging untersucht.

Abbreviations

BA	Broca's area
BC	brain code
BST	bed nucleus of the stria terminalis
BSTL	bed nucleus of the stria terminalis, lateral part
BSTLC	bed nucleus of the stria terminalis, laterocentral subdivision
BSTLD	bed nucleus of the stria terminalis, laterodorsal subdivision
BSTLP	bed nucleus of the stria terminalis, lateroposterior subdivision
BSTM	bed nucleus of the stria terminalis, medial part
CeA	central amygdaloid nucleus
CRF	corticotropin releasing-factor
HPA	hypothalamic-pituitary-adrenal
MeA	medial amygdaloid nucleus
MNI	Montreal Neurological Institute
MR	magnetic resonance
MRI	Magnetic Resonance Imaging
PET	Positron Emission Tomography
PLI	Polarized Light Imaging
SI	substantia innominata
VTA	ventral tegmental area

List of Figures

1 Introduction

Most human brain maps provide information of cortical and main subcortical regions, but not about small subcortical structures, as those in the basal forebrain. In addition, they rarely provide 3D-information, and usually do not include any data about intersubject variability. Even detailed maps have difficulties representing accurate information of structures with complex shape and variable appearance. The exact shape, location and full extent of these structures can only be inferred from such atlases (see e.g. Mai et al. (2007)).

This work presents the serial mapping of the bed nucleus of the stria terminalis (BST), a gray matter structure of the basal forebrain, over its whole extent and also of its cytoarchitectonic four subidivisions by providing high-resolution three-dimensional reconstructions. Interindividual variability will be considered by computing probabilistic maps in a common three-dimensional reference space.

This chapter will introduce the bed nucleus of the stria terminalis, providing details about its fiber architecture, functional aspects and blood supply. Aims and objectives will be explained at the end of this chapter. After a brief description of how histological sections were processed, cytoarchitectonical mapping and border definitions to neighboring structures will be explained. The Chapter Results (page 15) presents the cytoarchitectonic features of each of the subdivisions, the 3D reconstruction and the probabilistic maps. In the Chapter Discussion (page 25) results will be compared with previous studies. In the last chapter (page 29), two different modalities, addressing fiber and molecular architecture of this region will be presented as an outlook for further studies.

1.1 The bed nucleus of the stria terminalis

The BST, in some literature also abbreviated as 'BNST' or 'NIST', is an aggregation of several nuclei adjacent to the stria terminalis, deep in the basal forebrain at the level of the decussation of the anterior commissure. According to the literature, the BST can be divided into several subdivisions, depending on morphological, chemoarchitectonical or hodological criteria. Whereas Martin et al. (1991) suggested five subdivisions, Heimer

et al. (1999) wrote about only two parts with several subnuclei and Walter et al. (1991) and Mai et al. (2007) finally divided the human BST into three main parts. Although different authors came to various findings regarding the amount of subnuclei and further divisions, they seem to be quite consistent about the fact that the border definition of this particular basal forebrain structure is not at all easy to define. This might be caused by the heterogeneous appearance of some subdivisions and even by the challenging differentiation from adjacent structures, such as nucleus accumbens or septal nuclei on the rostral end or the hypothalamus or ventral pallidum at the caudal end of the BST. These challenges will be described in more detail below (Chapter 2.2.2).

1.1.1 Nomenclature

Early developmental investigations of Johnston (1923) suggested a relationship between the stria terminalis and its adjacent gray matter structure with the olfactory nuclei as well as connections to the amygdaloid complex. At that time, in the early 20^{th} century, the bed nucleus was not named yet, but Johnston referred to "the stria terminalis imbedded in a mass of gray which varies in volume and density at different levels" and later on it was considered as the "bed of stria terminalis" (Johnston, 1923). Brockhaus (1942) included the bed nucleus into his concept of "fundus striati", which involved besides the nucleus accumbens also the bed nucleus. As did Andy and Stephan (1968), who suggested the BST to be a caudal part of the septal nuclei, but already named the structure bed nucleus of stria terminalis.
This thesis will mainly follow the nomenclature of Heimer et al. (1999) and deOlmos (2004), who divided the BST into two main parts, the lateral and medial BST. That was supported by early developmental studies of Johnston (1923) and has been used by other well-known investigators of this region. Divergent from Heimer's naming herein will be the oval subdivision, which is called BSTLC in this thesis instead of Heimer's suggestion of "BSTLDcn".
The name of the sublenticular area of the BST is very inconstistent among authors. Early studies refer to that zone as substantia innominata (SI), as it was difficult to define the exact boundaries of these structures on histological images. Different authors not always refer to the same structures when using the term SI. Martin et al. (1991) for expample includes the ventral pallidum, the nucleus basalis of Meynert and the entire subcommissural region within the SI. This is similar to the suggestion of Heimer and van Hoesen (2006), who added the ventral striatum and the extended amygdala to the system, as already suggested by Alheid and Heimer, recommended in 1988.

1.1.2 The extended amygdala concept

The concept of the extended amygdala states that the amygala has cellular connections to the BST and its adjacent stria terminalis as well as to the substantia innominata (Heimer and van Hoesen, 2006). It has been well-described and received broad acceptance throughout the whole scientific community. Johnston (1923) described a linkage between the basal forebrain, including the BST, the SI and the amygdala, its central and medial nuclei, respectively, but not the laterobasal amygdala (Martin et al., 1991). The concept suggests that the division of the amygdaloid nuclei into a medial and lateral

part is also applicable to the BST as it is to the SI and the small cellular band adjacent to the stria terminalis connecting the supracapsular BST and the amygdala. According to developmental findings the bed nucleus has indeed been divided into a lateral and medial subdivision (Johnston, 1923).
The bed nucleus with its various subdivisions is most prominent at the decussation of the anterior commissure and its dorsal cell column runs adjacent to the stria terminalis alongside the ventricular surface of the thalamus. Besides, it has ventral sublenticular extensions towards the central amygdaloid nucleus (CeA), which was first detected by deOlmos and Ingram (1972). Not only cytoarchitectonic (McDonald, 1983) similarities between the BST, the central and medial amygdaloid nucleus, but also histochemical (deOlmos and Ingram, 1972) and immunocytochemical (Woodhams et al., 1983) consistencies have been observed in rats, which all led to strong acceptance of the extended amygdala concept. These studies were compared and confirmed by Martin et al. (1991), who included human and monkey data in his study. The concept is supported by continuous parcellation based on cytoarchitectonic and chemoarchitectonic criteria, most of all for immunoreactive neurons and fibers containing the neuropeptide leucin-enkephalin (Martin et al., 1991). In particular, there are similar patterns of cell types but also of neuropeptides in the centrolateral part of the CeA as it was found in the laterodorsal subdivision of the BST. These findings were similar to the continuum of the medial part of the BST and the medial amygdaloid nucleus, although the immunoreactivity there was less expressed (Martin et al., 1991).

1.1.3 Afferent and efferent projections

According to the extended amygdala concept, there are several fiber bundles connecting the BST with the amygdaloid complex. Moreover, there are fiber connections from and to several cortical (limbic and insular cortex) and subcortical regions and to certain brainstem nuclei (Di Marino et al., 2016).
Afferent connections reach the BST mostly from the amygdala, especially the central amygdaloid nucleus (CeA), but also from the cortex, hypothalamus and some brainstem centres (Di Marino et al., 2016) as well as some fornical fibers (Nieuwenhuys et al., 2008). Most fibers run from the lateral part of the CeA through the stria terminalis reaching the lateral part of the BST (Petrovich and Swanson, 1997). On a more caudal level they also run to parts of the SI, whereas there are only few connections from the nucleus accumbens in more rostral sections (Petrovich and Swanson, 1997). In addition, the medial amygdaloid nucleus (MeA) projects to the medial part of the BST, which is also in accordance with the extended amygdala concept (Di Marino et al., 2016), as were connections from the anterior medial preoptic nucleus, the medial amygdaloid nucleus and the posterior part of the BST itself to the medial part of the BST found (Lebow and Chen, 2016). Apparently, cortical, lateral, baso-lateral and baso-medial amygdalar nuclei have almost no influence on BST-afferents (Petrovich and Swanson, 1997). However other authors state, that there are indeed important afferents, at least from the laterobasal amygdala projecting to the oval subdivision of the BST (Dabrowska et al., 2016; Kim et al., 2013), or fibers running from the laterobasal amygdala towards the CeA to the lateral part of the BST (Davis et al., 2010).

The infralimbic cortex as well as the adjacent dorsal peduncular cortex project to the BST, but also through the SI to the medial and central amygdaloid nuclei. Whereas there are strong and moderate infralimbic connections to the medial and to the posterior part of the BST, there are only minor projections to the dorsal part of the BST (McDonald et al., 1999). There are also strong connections from the prelimbic cortex to the posterior part of the BST, projecting to the SI.

There are several fiber pathways running from the BST to different target regions of the human brain. The most prominent projection of the BST runs alongside the stria terminalis, adjacent to the anterior horn of the lateral ventricle, caudate nucleus and the ventricular surface of the thalamus, terminating in the central and medial amygdaloid nuclei and finally in the medial prefrontal cortex (Krüger et al., 2015). Other pathways run towards the hypothalamus to the amygdala and across the anterior commissure, the transition zone between caudate nucleus and nucleus accumbens, finally terminating in the frontal lobe, namely in Broca's area (BA) 10 and BA 11 (Krüger et al., 2015). Other studies of human BST pathways suggest efferent connections to the temporal pole and the paracingulate gyrus (Avery et al., 2014). Interestingly, the hypothalamus receives inputs only from the anterodorsal part but not from the oval subdivision of the BST (Kim et al., 2013). Studies with mice, rats and cats revealed that there are also efferent connections to the raphe nuclei, the paraventricular nucleus of the hypothalamus and the ventral tegmental area (VTA) of the mesencephalon (Dabrowska et al., 2016; Dong et al., 2001; Holstege et al., 1985).

Like afferent connections, efferent projections also show a remarkable consistency with the extended amygdala concept: the medial BST and its medial sublenticular extended amygdala project to the medial substantia nigra (pars compacta), whereas the lateral BST as its lateral sublenticular extended amygdala reach the mediolateral substantia nigra, the pars reticulata (Fudge and Haber, 2001). These findings were supported by Dabrowska et al. (2016) who found projections from the oval subdivision, which is a part of the lateral BST, to the substantia nigra reticulata.

1.1.4 Function

The extended amygdala concept becomes noticable again in functional aspects, as the central amygdaloid nucleus and the BST are both involved in fear and anxiety responses (Davis et al., 2010), as corticotropin releasing-factor (CRF) is released and the hypothalamic-pituitary-adrenal (HPA) axis is activated. Differences between these two structures were pointed out recently, though: Whereas the CeA causes defensive reactions to immediate or cued threat situations, the BST causes responses on diffuse threats, occuring in sustained fear (Gungor and Paré, 2016; Lebow and Chen, 2016). Another study revealed that the BST and the insular cortex are both activated in situations of imminent threats, but not the amygdala (Somerville et al., 2010). Anxious individuals seem to have even higher activities in these regions and are more vigilant than normal people (Somerville et al., 2010). The authors of a similar study found out that patients with generalized anxiety disorder show an increased activity in the BST

in situations of uncertainty and sustained fear, whereas the amygdala's activity is decreased (Yassa et al., 2012). The authors of the latter study suggest that the activity of the amygdala might be suppressed in sustained fear and stress in order to maintain the higher activation of the BST (Yassa et al., 2012).
Furthermore, the BST is known to be involved in endocrine functions, influencing reproduction and the circadian rhythm. The BST and other basal forebrain structures and the brainstem contain gonadal steroid-receptive neurons, influencing the hormonal balance of estrogen and androgen (Nieuwenhuys et al., 2008). BST and CeA are as well influenced by the daily expression of the circadian clock gene PER2 regulated by the suprachiasmic nucleus, which also influences apart from the circadian rhythm also hormonal and emotional states (Amir and Stewart, 2009).

It is believed, that several subdivisions of the BST are also responsible for different functions. The lateral BST for example is known to be involved in anxiety and in addiction circuitries (Torrisi et al., 2015). The encapsulated oval subdivision of the BST has drawn attention throughout papers dealing with the BST (Avery et al., 2016; Dabrowska et al., 2016; Gungor and Paré, 2016). It is expected that the oval subdivision is dependent on afferents from brainstem nuclei, periaqueductal gray or the insula, which are responsible for anxiogenic signals in the brain and that CRF containing neurons are activated within anxiety modulation in the BST (Dabrowska et al., 2016; Amir and Stewart, 2009).
According to Kim et al. (2013) different subdivisions can even cause opposite functional effects: The oval subdivision, as just mentioned is involved in anxious situations. In contrast, the anterodorsal subdivision, surrounding the oval BST, modulates a decreased avoidance of risk as a lower respiratory rate, which was considered as an anxiolytic reaction.

As Davis et al. (2010) suggested that electrolytic lesions of the CeA influcence the connection between the laterobasal amygdala and the bed nucleus of the stria terminalis, lateral part (BSTL), and therefore a dysfunction results in a disconnection between the CeA and the BST, but also between the laterobasal amygdala and the BST (Davis et al., 2010), which can also result in alteration of the HPA axis. Impairment of the BST might result in alterating reproductive behavior or social anxiety (Lebow and Chen, 2016).

1.1.5 Blood supply of the bed nucleus

The BST receives its blood mainly from the anterior cerebral artery. Five branches from medial, lateral, dorsal and two from ventral direction supply different subdivisions of the BST. Although this classification sounds reasonable when separating the BST, they do not equally correspond to the cytoarchitectonically delineated subdivisions of the BST (Danics et al., 1985). According to studies of the rat, the lateral arteries joining the BST from its rostral and its caudal end are the most developed arteries (Danics et al., 1985). These branches derive as well from the anterior cerebral artery, supplying the lateral preoptic area and later on also the lateral BST, one branch entering from the rostral end, another one from its caudal end. The venous system is similar built, whereas only

four different branches drain the BST from its medial, lateral, dorsal and ventral part into the major basal veins (Danics et al., 1985).

1.2 Other basal forebrain structures

As border detection in the basal forebrain is challenging, it is important to have good knowledge about neighboring structures, which shall be briefly described in this section. The human basal forebrain lies medial in the human brain at the level of the anterior horn of the lateral ventricles and the anterior commissure. It is extending to olfactory structures on the ventral and medial brain surface. The ventral forebrain consists of a variety of structures, where the BST-amygdala continuum is one part of it (Martin et al., 1991). Other structures are the magnocellular complex, the ventral striatopallidal system as well as preoptic and anterior hypothalamic areas.
Most prominent magnocellular regions in the basal forebrain are the nucleus of the diagonal band of Broca and the nucleus basalis of Meynert extending from the dorsomedial part of the forebrain to its lateroventral part. These structures are often included in the term SI and contain large, darkly-stained cholinergic neurons (Heimer et al., 1999). The nucleus basalis of Meynert is considered to decrease in size within ageing brains and therefore is an important factor for structural changes in Alzheimer's disease or other neurodegenerative disorders (Zaborszky et al., 2008). Due to their magnocellular darkly stained neurons, these regions are clearly distinguishable from other basal forebrain structures. The nucleus of the horizontal limb of the diagonal band has as the BST connections to the MeA and CeA (Nieuwenhuys et al., 2008).
The ventral striatum, mainly comprising of the nucleus accumbens, is located ventrally to the anterior limb of the internal capsule and also ventral of the anterior commissure. On coronal sections it seems to be merging with its dorsal part, the caudate nucleus. Following subsequent sections in caudal directions, these two structures diverge and in between the bed nucleus appears. The ventral pallidum is analogous to the ventral striatum. These two structures can also be combined to the ventral striatopallidal system (Heimer et al., 1999).
The preoptic area contains small neurons and has no distinct cytoarchitectonic borders to its adjacent lateral hypothalamic area (Baroncini et al., 2012). Medially, though, it can be distinguished from the paraventricular nucleus of the anterior hypothalamic area, due to its magnocellular component adjacent to the third ventricle. The fornical part of the paraventricular nucleus borders the BST medially and the lateral hypothalamic area ventrally in caudal sections of the BST (Baroncini et al., 2012). The anterior hypothalamic area comprises of the darkly stained suprachiasmatic and supraoptic nuclei, the aforementioned paraventricular nucleus of the hypothalamus with its fornical part and the lateral hypothalamic area. Both, the anterior and lateral hypothalamic area are adjacent to the BST (Baroncini et al., 2012).
Last but not least, numerous parvicellular neuronal islands are scattered throughout the whole basal forebrain. These islets, also known as "interface islands" or "intercalated islands", frequently appear at the borders of ventral striatum, ventral pallidum but also within the lateral bed nucleus of the stria terminalis (Heimer et al., 1999).

1.3 Aims and objectives

The aim of this work is to analyze the cytoarchitecture, size and shape of the bed nucleus and its four subdivisions, to assess its intersubject variability, and to provide maps of these structures in 3D-space. This is accomplished by providing a detailed high-resolution 3D-reconstruction of each of the subdivisions and probabilistic, stereotactic maps. The latter are presented in the format of the Montreal Neurological Institute (MNI) reference brain (Evans et al., 2012). They can serve as a basis for future neuroimaging studies on the BST, but also as a reference source for clinical findings.

2 Methods

Ten postmortem human brains were obtained from the body donor program in accordance with the guidelines of the Ethics Committee of the University of Düsseldorf (see Fig. 1). Five male and five female brains, age ranging from 30 to 85 (mean age: 57.8 years, SD=19.3) were chosen for this work. According to the clinical records there were no indications for neurological or psychiatric diseases. Postmortem delay ranged according to protocols from 10 to approximately 24 hours. For more details of the selected brains see Table 1.

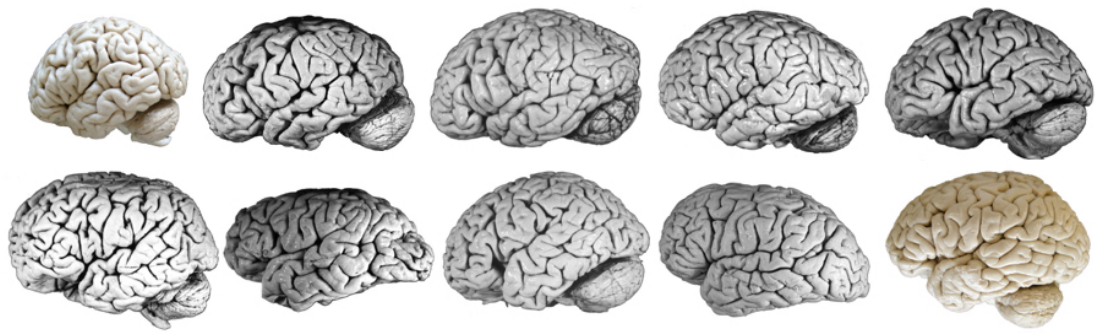

Figure 1: Ten postmortem human brains, left hemispheres, taken from the body donor program of the University of Düsseldorf.

2.1 Histological processing

The ten brains processed as described earlier in more detail (Amunts et al., 1999). In short, they were fixed in 4 % buffered formalin or in Bodian mixture, then dehydrated, embedded in paraffin and serially sectioned in coronal plane. Every 15^{th} section (each 20 µm thick) was mounted and stained for cell bodies with a modified silver method (Merker, 1983). In two of the ten brains every single section of the more than 7000 sections was processed. These brains will be referred to as 'BigBrains' within this thesis (Amunts et al., 2013). Staining and further processing of these brains were the same as in all other brains. The sections were mounted on histological glass slides to be fur-

Table 1: Postmortem brains used for cytoarchitectonical mapping

Brain code	Age [years]	Gender	Cause of death	postmortem time	Fresh brain weight
BC 01	79	female	Bladder carcinoma	~24 h	1350 g
BC 03	69	male	Cardiovascular disease	16 h	1360 g
BC 05	59	female	Cardiorespiratory insufficiency	24 h	1142 g
BC 07	37	male	Acute right heart failure	<24 h	1437 g
BC 08	72	female	Renal failure	12 h	1216 g
BC 10	85	female	Mesenterial infarction	14 h	1046 g
BC 12	43	female	Pulmonary embolism	not known	1198 g
BC 13	39	male	Death by drowning	10 h	1234 g
BC 20	65	male	Cardiac insufficiency	14 h	1392 g
BC 21	30	male	Bronchopneumia, Morbus Hodgkin	~24.8 h	1409 g

ther available for observation under the optical microscope (Zeiss Axiolab 40, achroplan objectives, magnifications 4x and 10x) to delineate the nucleus. The borders detected under the microscope were labeled on every 15^{th} section (on the BigBrain, BC 21 even on every 5^{th} section) on high-resolution flatbed scans (Scanner of Huron Technologies: TISSUEscope™ HS). Images had a resolution of 20 µm, except the scans of BigBrain BC 21, having a resolution of 1 µm. The 20 µm sections were loaded into the java-based in-house software called "sectiontracer" for subsequent digital delineation of the structures, whereas the 1 µm sections were processed in "MicroDraw", an in-house extention of an open source web application for annotation of high resolution data (Source: https://github.com/neuroanatomy/microdraw). Annotations of 1 µm sections were accomplished and coordinates of the selected landmarks were saved as text-files for further processing, namely the 3D-reconstruction and the generation of probabilistic maps, which will be described in Chapter 2.3.

2.2 Cytoarchitectonic mapping of the bed nucleus

The mapping of the present work is based on cytoarchitectonic criteria to detect borders of the bed nucleus and to its adjacent structures. Criteria and dorsal/ventral, lateral/medial or rostral/caudal border definitions are described below.

2.2.1 Cytoarchitectonic criteria

Several criteria based on cytoarchitecture were employed to distinguish the BST from its neighboring structures and to identify different subdivisons of this gray matter structure.

Criteria included size, shape, density or distribution of neurons and glial cells. The shape of BST-neurons varied among different subdivisions and were round or oval, fusiform or asymmetrically multipolar. Whereas fusiform or multipolar neurons had mostly clearly visible dendrites, round or ovalshaped neurons seemed to have almost none or only short ones. The distribution of neurons was considered either to be equal or clustered as in interface islands, previously described by Sanides (1957). Also the distribution and density of glial cells were an important factor, as this composition was different in various divisions. Finally the neuropil, which comprises of neurons in deeper layers of the sections and not clearly identifiable glial cells and fibers, was included in those cytoarchitectonic criteria. However, these characteristics might differ due to blood vessels of substantial size or artifacts caused by normal histological processing. BST criteria varied at these marginal areas, but could still be applied in general.

2.2.2 Definition of borders of the bed nucleus

As the name "bed nucleus" already infers, it is "embedded" between several structures of the basal forebrain. Borders of the BST were considered as following: In sections on the level of the decussation of the anterior commissure the BST is bordered dorsally by the caudate nucleus, ventrally by the anterior commissure, medially by the fornix and laterally by the internal capsule. In more rostral sections the ventral border of the BST is the nucleus accumbens and medially the BST is bordered by the septal nuclei. Together with the head of the caudate nucleus the nucleus accumbens is the rostral border of the BST. In caudal sections the dorsal border of the BST is the reticular thalamic nucleus, and the lateral hypothalamic area or parts of the medial preoptic nucleus are the ventral border. At sections of this level the perifornical nucleus as well as the fornical part of the paraventricular nucleus of the hypothalamus were considered as the medial border of the BST. The delineation on very rostral or far caudal sections of the BST was not easy to accomplish at 20 µm resolution images and therefore required an intense observation under the microscope.

As described in Chapter 1.1.1, the nomenclature is inconsistent among authors. Criteria and nomenclature herein mainly followed the findings of Heimer et al. (1999), which also supported the division of the BST into two main subnuclei, the lateral and medial part of the BST. Further background information, above all to include detailed knowledge of the basal forebrain were taken from Mai et al. (2007). The nomenclature of this author differs slightly, as he suggested five subnuclei of the same hierarchy instead of two. In addition, the thin cell band following the stria terminalis to the amygdala is not fully illustrated in this atlas. Cell bridges are only suggested on one page of the atlas, but are missing on the subsequent site. Nevertheless, these maps give a good insight into the basal forebrain organization.
The original purpose of this project was the delineation of the main part of the BST. As the appearance of this basal forebrain structure itself is very heterogeneous, it became evident to describe various subdivisions of the BST to set critieria for itself but also to compare those with adjacent, similar structures, such as the nucleus accumbens or the lateral hypothalamic area. Very thin cell bridges connecting the BST and the amygdala

on its sublenticular level were not included in this work, as these parts were very difficult, or even not at all detectable by cytoarchitetconical analysis. Also, these very small compartments would have been too small to include in probability maps.
Last but not least, it should be mentioned that this thesis addresses the mapping of the main part of the BST and the beginning of the thin band adjacent to the stria terminalis running dorsally to the BST, as this cell column merges with the posterior subdivision. This part (see also Chapter 1.1.2) could also be associated with 'the extended amygdala', but not to the main part of the BST. In order to show the detailed shape of the BST, sections with this part of the BST visible were included in the mapping.

2.2.3 Cytoarchitectonic observations in brain BC 07

During the mapping of brain code (BC) 07, it was noticed that some of the neurons appear bigger, round and less stained than in sections of the other nine postmortem brains. Those cells, in literature also known as "ballooned cells", were quite frequent in subdivisions of the BST containing abundant fiber material, like in the central or posterior subdivision, respectively, but appeared in every subdivision of the BST (Fig. 2). They were also found in other subcortical structures, such as the lateral hypothalamic area or septal nuclei. When verifying other compartments of the brain, e.g. cortical areas in the temporal or frontal lobe, the amygdala, or the hippocampus, no or only a minor amount of ballooned cells could be detected there. The reason for these swollen cells of this particular brain is unknown, as the medical record did not show any indication. As the ballooned cells did not seem to have any impact on the shape or volume of the BST, it was not excluded within this study.

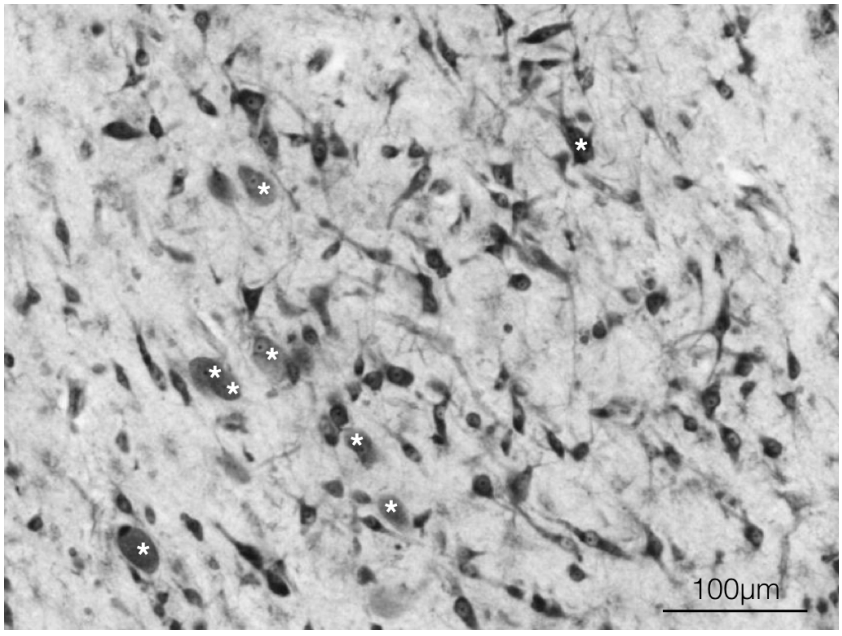

Figure 2: Ballooned cells (asterisks) of bigger size, shape and lighter staining than normal neurons in brain BC 07. Scale bar 100 µm

2.3 3D-reconstruction and generation of probabilistic maps

Magnetic resonance (MR) images were taken from the fixed postmortem brains before paraffin-embedding and subsequent processing. In addition, digital images of the stained histological sections were acquired. These two data sets were used to remove shrinkage, deformations or other artifacts obtained during histological processing and to achieve a high-quality image registration and 3D-reconstruction (Amunts et al., 1999). The registration process was initially performed linear affine, which was followed by an alignment driven by the local gray level difference between the template and reference data set and a final non-linear transformation.
Mapping of the BST and its four subdivisions was performed on serial, histological sections in both hemispheres in ten brains. In total, 462 sections were analyzed and further processed. To label the extent the in-house software "sectiontracer" was used (see Chapter 2.1). Volumes were calculated by the contours of the nuclei in images at a resolution of 20 µm in-plane (Amunts et al., 2007). The volumes were corrected by their corresponding shrinkage factor. Volumes of each subdivision were then normalized using the individual brain volumes to detect putative interhemispheric and/or gender differences.

The reconstruction in three-dimensional space was performed at two levels to analyze the complex topography of the BST and its subdivisions with two different spatial resolutions: First, sections with a resolution of 1 µm of one BigBrain (BC 21) was downsampled and transformed to 20 µm (Mohlberg et al., 2016). Every fifth section (distance between sections: 100 µm) of the BigBrain was mapped to 3D-reconstruct images with high spatial resolution of 100 µm, and to build a surface allowing to identify the detailed shape of the structure. Secondly, reconstructions of the 3D-reconstructions of all ten brains were registered to the Colin27 T1-weighted single-subject template brain of the MNI with a spatial resolution of 1 mm (Evans et al., 1992, 2012) and further aligned to the anatomical MNI space (Amunts et al., 2005). Data of all ten brains were superimposed in this reference space to obtain probability maps.
As the BST is a very small structure, regarding the spatial resolution of the reference space, we decided to combine the three subdivisions of the lateral bed nucleus (BSTL) into one probability map. A second probability map was computed for the medial part (bed nucleus of the stria terminalis, medial part (BSTM)), which is also in accordance with the extended amygdala concept (Chapter 1.1.2). The probabilistic maps show the frequency of the BST in each voxel of the MNI reference space, ranging from 0 to 100 %. Blue colors indicate that only one brain of ten is located in a particular area; red colors refer to ten brains out of ten overlap in this region. The resolution of these probability maps is 1 x 1 x 1 mm. Further details on the generation of the probability maps can be read in Bludau et al. (2014).

3 Results

The mapping of the bed nucleus of the stria terminalis and its subdivisions based on cytoarchitectonic criteria is presented within this chapter. After a brief description of how criteria were applied to delineate the BST and its identified subdivisions (Chapter 3.1.1), a high-resolution 3D-reconstruction followed by probabilistic maps of the lateral and medial part of the BST will be shown at the end of this chapter (Chapter 3.3 and 3.4).

3.1 Cytoarchitecture of the bed nucleus

The BST is embedded between various white matter structures of the basal forebrain, such as the anterior commissure, internal capsule and fornix and is adjacent to the anterior horn of the lateral ventricle close to the midline (Fig. 3 a, b). It appears ventrally enlarged and dorsally elongated on most coronal sections. In more rostral sections its shape becomes more compact (Fig. 4 a) and its cytoarchitecture gets very similar to the one of its adjacent nucleus caudatus and nucleus accumbens. On caudal sections, however, the extent to the stria terminalis becomes visible as a very thin band growing towards the caudate nucleus and the anterior thalamic nuclei, which gives it a very narrow and elongated shape (Fig. 4 d, e). As mentioned before, the sublenticular part of the BST was not included in these results, as well as the whole supracapsular band and the stria terminalis running side by side towards the amygdala. Following the course of the BST in serial sections not only the remarkable structure changes in shape during its rostrocaudal extent, but also its subdivisions show an immense variation (Fig. 4).

3.1.1 The four subdivisions of the bed nucleus

According to cytoarchitectonic criteria and border definitions described above (Chapters 2.2.1 and 2.2.2), four different subdivisions were identified and traced in serial sections (Fig. 3). Three of them were found to be part of the lateral division, i.e. bed nucleus of the stria terminalis, laterocentral subdivision (BSTLC), bed nucleus of the stria terminalis, laterodorsal subdivision (BSTLD), bed nucleus of the stria terminalis, lateroposterior subdivision (BSTLP) and the fourth was the medial part of the bed nucleus (BSTM). All subdivisions have their characteristic features, which are described below.

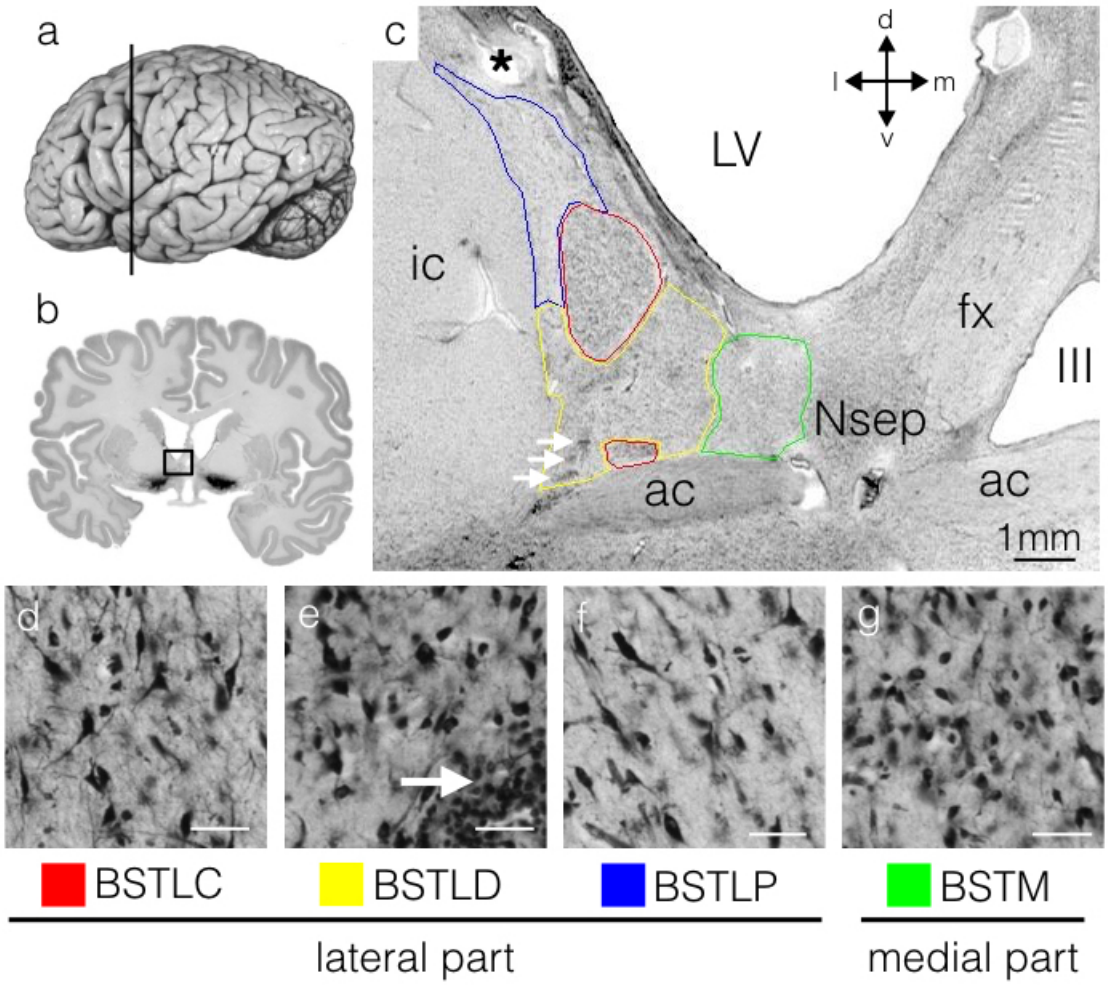

Figure 3: Four subdivisions of the bed nucleus of the stria terminalis and their cytoarchitecture. (a) Lateral view of a postmortem brain, left hemisphere. (b) Cytoarchitectonic coronal section at the level marked in a. (c) Magnification of the region of interest enclosed in black in b showing four different subdivisions of the bed nucleus of the stria terminalis (BST): Three regions of the lateral part, BSTLC (red) – central part, BSTLD (yellow) – dorsal part, BSTLP (blue) – posterior part and medial part – BSTM (green). Directions: dorsal (up), ventral (down), lateral (left) and medial (right). (d)-(g) Magnifications of each corresponding subdivision, scale bar 50 µm. White arrows mark parvicellular islands in c and e. Asterisk marks the thalamostriate vein in c. Abbreviations: ac - anterior commissure, fx - fornix, ic - internal capsule, LV - lateral ventricle, Nsep - nucleus septalis, III - Third ventricle.

The lateral part of the bed nucleus of the stria terminalis

The lateral part of the BST was further divided into three parts: Central, dorsal and posterior. This subnucleus is adjacent to a large number of blood vessels of various size. The most prominent is the thalamostriate vein (see Fig. 3 c, asterisk), which appears at the dorsomedial border of the BST, very close to the lateral ventricle and the caudate nucleus, but also runs through some subdivisions of the BST.

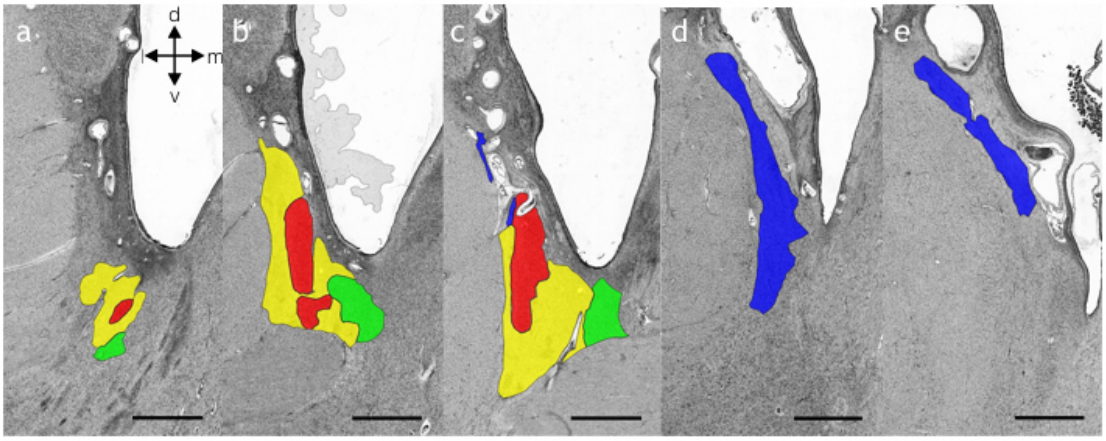

Figure 4: The bed nucleus in serial histological sections from its rostral (a) to its caudal end (e). Distance between two images is approximately 1.2 mm, which corresponds to every 60^{th} section. Red: BSTLC, yellow: BSTLD, blue: BSTLP and green: BSTM. Directions: dorsal (up), ventral (down), lateral (left) and medial (right). Scale bar: 2 mm.

The **laterocentral part** (BSTLC) has an oval shape in coronal sections and contains mostly triangular shape of medium-sized neurons as its main characteristics (Fig. 3 c, d). Due to its consistent shapes of neurons and the translucent background, caused by the minor amount of glial cells, it is the most homogeneous subdivision of the BST. Neurons do not follow any particular orientation and their nucleus is usually lightly stained and clearly distinguishable from the darkly stained nucleolus. The BSTLC is encapsulated by a thin band, appearing very brightly in cytoarchitectonical sections and can be recognized even at low magnification of the microscope. It has a very scarce and lucid background, due to the small number of glial cells.
The BSTLC mostly keeps its oval shape from its rostral to its caudal end (Fig. 4 a, b, c). One or two small structures revealing the same cytoarchitectonic pattern as it was known from the main BSTLC subdivision were found and separately delineated. A decrease of the distance between two sections from 15 to five in BC 21 revealed that those islands are connected with the main oval-shaped subdivision of the BSTLC. Figure 5 shows three subsequent sections: two areas isolated from the main structure, shown in Figure 5 (a), that were found ventral and ventromedial of the main part of the BSTLC, are merging on Figure 5 (b). Figure 5 (c) shows both of the islands fused with their main subdivision to result in one big BSTLC, but also a new island is separated on its medial border. Note that this cytoarchitectonical pattern is different from the one of parvicellular interface islands (Fig. 5, arrows), known from the BSTLD and described in the following paragraph.

The **laterodorsal part** (BSTLD) almost completely covers the BSTLC. It is characterized by numerous clustered neurons (Fig. 3 c, e), also known as "interface" islands, (see Chapter 1.2). Most of these islands occur at the level of the decussation of the anterior commissure, right above this fiber bundle and between the internal capsule and the

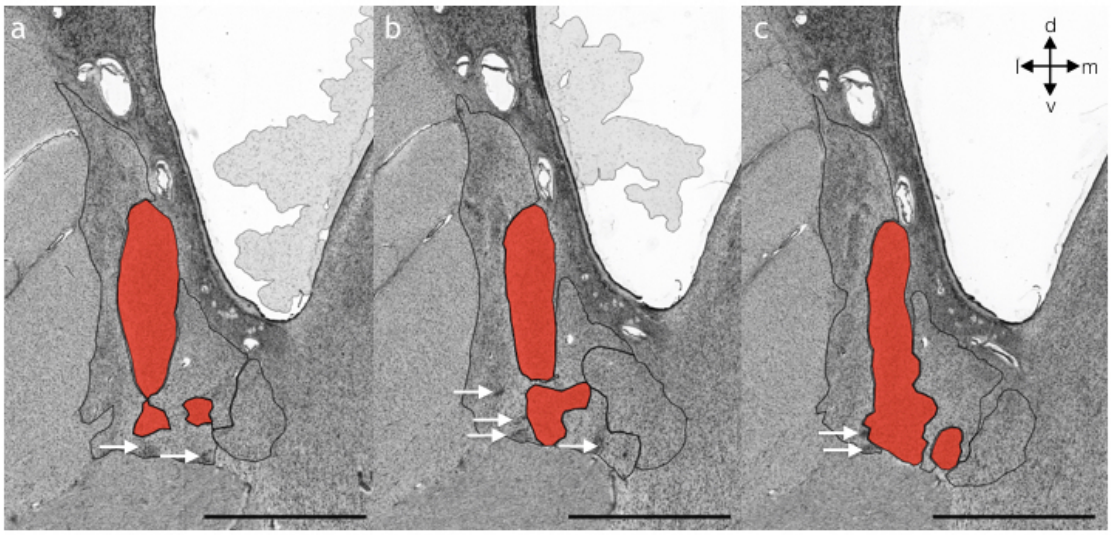

Figure 5: Oval shaped subdivision of the bed nucleus (BSTLC) showing three neighboring sections, left hemisphere. (a) Two islands of the red laterocentral part of the bed nucleus (BSTLC) are separated from the main oval-shaped area. (b) The islands start to fuse. (c) The two islands of (a) are totally merged with the other part of the BSTLC, but simultaneously another island appeared on the medial side. Arrows point to parvicellular interface islands of the BSTLD (laterodorsal part of the BST), having a different cytoarchitectonical pattern. Distance between two sections approximately 100 µm, which correspond to 5 sections. Directions: dorsal (up), ventral (down), lateral (left) and medial (right). Scale bar 2.5 mm.

BSTLC. Neurons in these clusters are in contrast to the BSTLC more densely packed, more darkly stained and of round and not triangular shape. Additionally, the interface islands were not encapsulated by a fiber band. Between those cell aggregates neurons of the BSTLD are mediumsized, mostly fusiform and have a dorsoventral direction of orientation.

Finally, the **lateroposterior** part (BSTLP) gradually replaces the BSTLD. It contains both darkly stained medium-sized neurons and lighter stained small neurons (Fig. 3 c, f). It contains already numerous fibers of the stria terminalis and merges with this fiber bundle at its dorsal extention towards the caudate nucleus. This subdivision comprises granular interface islands at the border to the internal capsule, as does the BSTLD, although in considerably fewer amount. The neurons of the BSTLP show as well a dorsoventral orientation of mostly fusiform shape. The BSTLP elongates dorsally on caudal sections, as a narrow band can be observed growing towards the caudate nucleus (Fig. 4 d, e). On its ventral border this subdivison gets scattered and tend to have very thin digitate extentions towards the substantia innominata, which were not visible in everey brain, though.

The medial part of the bed nucleus of the stria terminalis

The BSTM contains varying shapes of neurons, which lead to a very heterogeneous cell population: Small and densely packed neurons of round shape as medium-sized multiform neurons are characteristic for this subdivision (Fig. 3 c, g). The staining and the amount of glial cells vary in this subdivision, it has areas poor in glial cells fading into glial cell-rich areas. In general, smaller neurons are less stained, whereas larger neurons are more darkly stained. The density of neurons of the BSTM increases in caudal sections.

3.1.2 Variation in size

In some brains blood vessels, which most likely branch from the thalamostriate vein, directly run through the BST and seperated it into two or more parts (Fig. 6). In some cases this led to considerable changes in size (Fig. 6 a, b), whereas other cases only showed minor incisions (Fig. 6 c-e). BSTLC and BSTLD were the subdivisions most often affected by this phenomenon. BSTLP and BSTM contained only blood vessels of neglectable size that had no influence on the size of the subdivisions. The impact is not always the same in both hemispheres of the same brain, as (a) and (d) of Figure 6 can be compared.

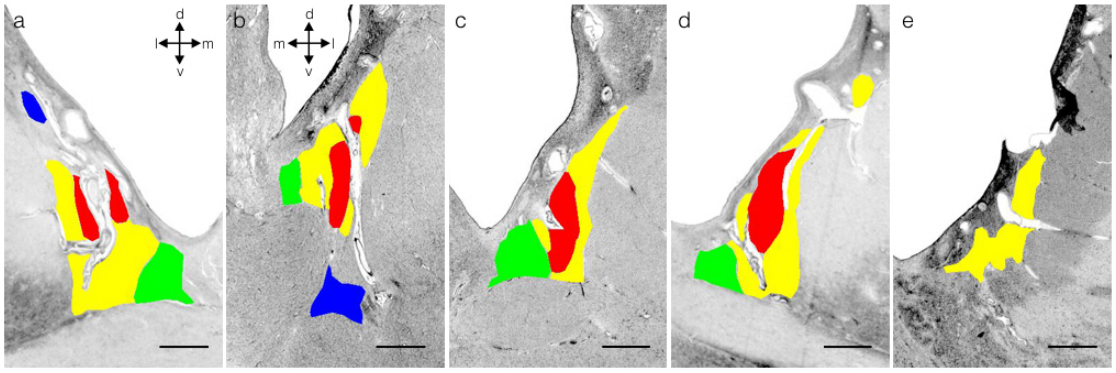

Figure 6: Vascular architecture and bed nucleus in sections of four different brains (a) to (e). (a) and (d) belong to the same brain. (a) is a BST of the left hemisphere, directions: dorsal (up), ventral (down), lateral (left) and medial (right), (b) to (e) are bed nuclei of a right hemisphere, directions: dorsal (up), ventral (down), lateral (right) and medial (left). Red: BSTLC, yellow: BSTLD, blue: BSTLP and green: BSTM. Scale bar 1 mm.

3.2 Size of the bed nucleus

The mean volume of the whole BST is 74.3 mm^3 (SD=11.0) for the left and 73.3 mm^3 (SD=14.2) for the right hemisphere. The volume of each brain and subdivision can be seen in Figure 7; they show a remarkable interindividual variability. In some brains the largest subdivisions, BSTLD and BSTLP have similar volumes (BC 08, BC 12), whereas in other brains the BSTLD is almost twice as large as the BSTLP (BC 03, BC 20).

In all brains BSTLC and BSTM are substantially smaller than the other subdivisions. Normalized volumes showed no significant differences between hemispheres or sex.

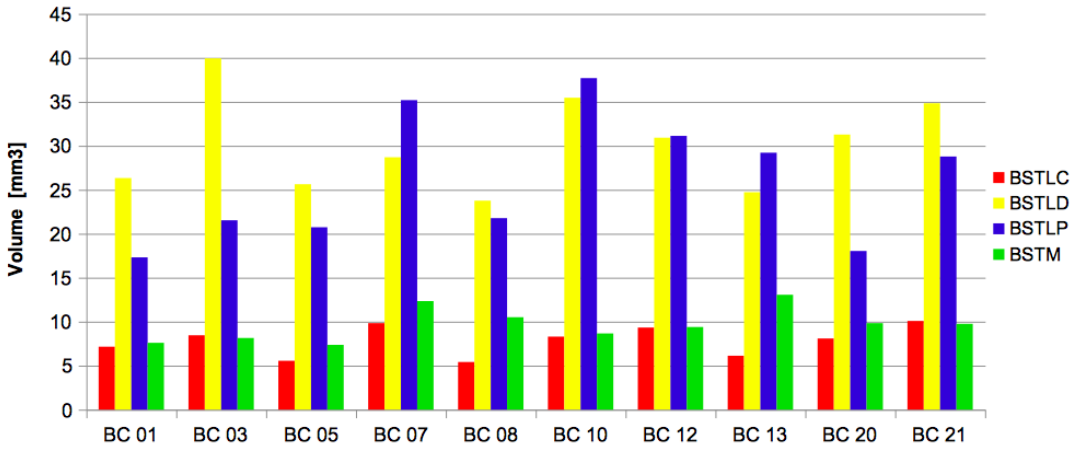

Figure 7: Corrected volumes of each brain and subdivision. As there were no hemispheric differences, the mean value of each subdivision of both hemispheres is reported.

3.3 High-resolution 3D-reconstruction of the bed nucleus

In order to better understand the complex shape oft he BST in 3D, a high-resolution 3D-reconstruction of the BST based on every 5^{th} delineated section was performed. Figure 8 shows the four subdivisions from medial (a) and rostral (b) view. It should be emphasized that the red BSTLC is in fact bigger than it appears in this figure, as it is almost fully covered by the yellow BSTLD. Only small parts of the BSTLC are exposed. The BSTLP was revealed to be the biggest subdivision, displaying an elongated and narrow shape. Thinned elongations in ventral direction in both images of Figure 8 as rudiments of the sublenticular part of the BSTLP can be observed (arrows). In (b) of the same figure, the curvature of the dorsal, supracapsular BSTLP can be seen. The indentation in (a), marked by an asterisk, indicates where the enclosed anterior commissure would be located.

In order to reveal the shape of the almost fully covered BSTLC this subdivision is illustrated with the surrounding BSTLD, which is visualized transparent (Fig. 9). From mediorostral view the oval shape can be recognized in Figure 9 (a). The caudal view (Fig. 9 b) unveils that the BSTLC has bulges extending in medial direction. In both images separated islands of the BSTLC, depicted in red, are visible.

3.4 Probabilistic maps of the bed nucleus

Registration of the delineated structures onto the MNI reference brain template and the subsequent superimposition of all ten brains resulted in probabilistic maps (Figs. 10,

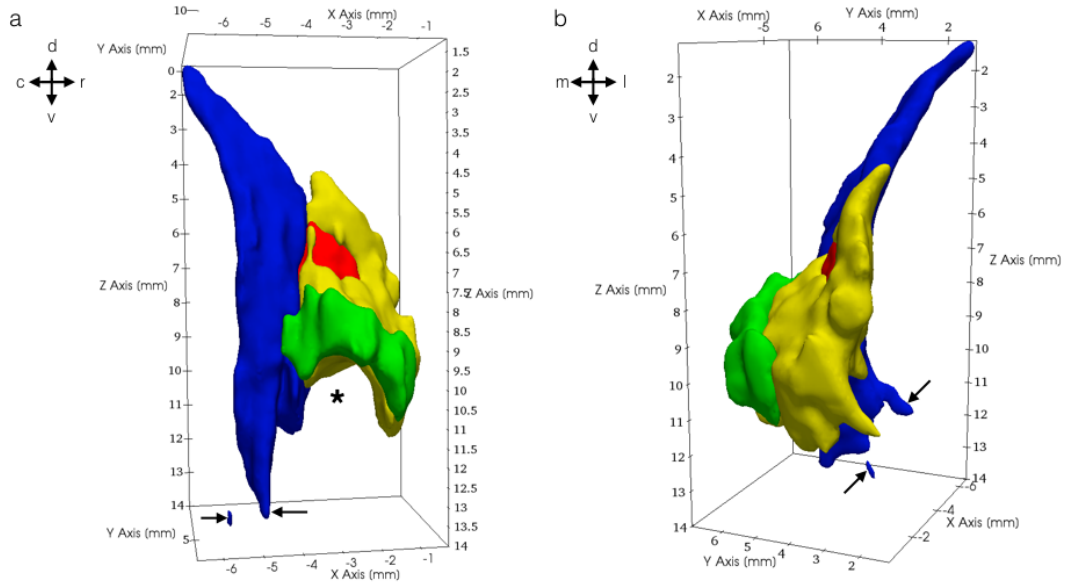

Figure 8: High-resolution 3D-reconstruction of four subdivisions of the bed nucleus. (a) Medial view. Directions: dorsal (up), ventral (down), caudal (left) and rostral (right). (b) Rostral view. Directions: dorsal (up), ventral (down), medial (left) and lateral (right). Arrows show sublenticular rudiments of the BST. Asterisk in (a) indicates the position of the anterior commissure. Red: BSTLC, yellow: BSTLD, blue: BSTLP and green: BSTM.

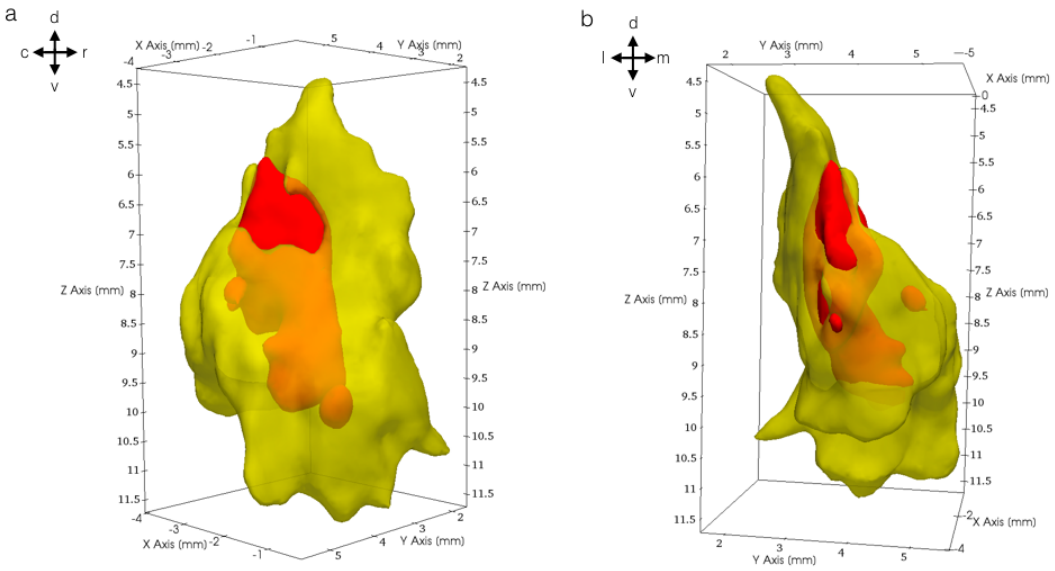

Figure 9: High-resolution 3D-reconstruction of BSTLC (red) and BSTLD (yellow). (a) Mediorostral view. Directions: dorsal (up), ventral (down), caudal (left) and rostral (right). (b) Caudal view. Directions: dorsal (up), ventral (down), lateral (left) and medial (right).

11). These maps show the location and extent of both subnuclei of all ten brains for all voxels of the reference brain. Regions of high overlap up to 100 % are colored in orange and red, meaning nine or even ten brains out of ten could be traced in the same region of the brain and represent therefore a high interindividual variability. Blue colors indicate a very small overlap showing percentage of 10 %. To get an overview about the representation of the subdivisions in all three dimensions, not only the coronal plane, which was used for delineation, is presented here, but also sagittal and axial planes are provided. The elongated and slightly curved shape of the BSTL is recognizable in coronal and sagittal planes (Fig. 10 at y = -1, y = -4, x = -8). Levels in coronal and sagittal plane indicate, that the bed nucleus hardly changes its shape in the dorsal part of the BSTL. On the axial plane it can be seen that the diameter of the BST is always oval to round (Fig. 10 z = 7, z = 13). The BSTM mainly keeps its shape, but is substantially smaller compared to the BSTL (Fig. 11).

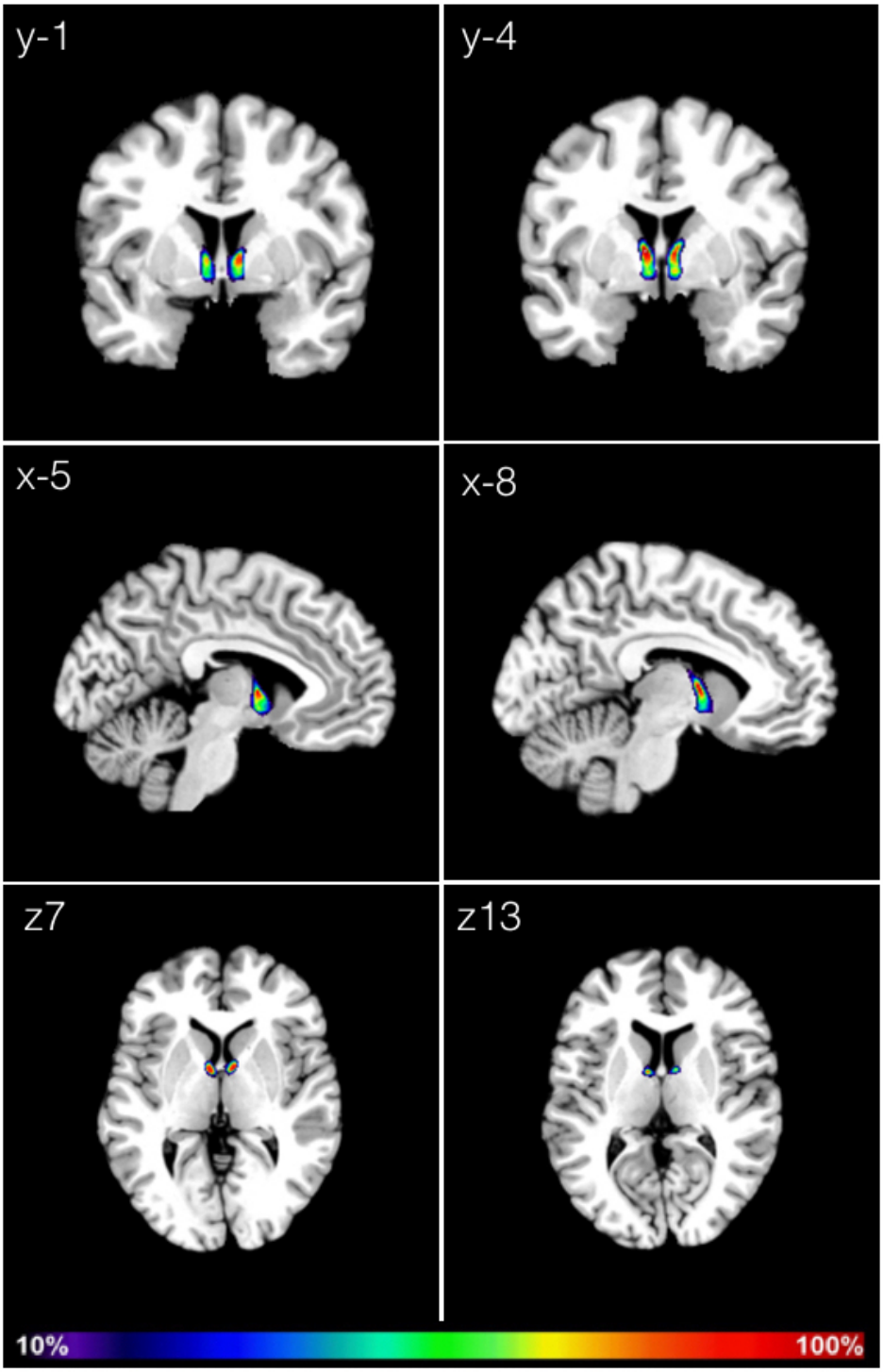

Figure 10: Probabilistic maps of the lateral part of the BST in coronal (top), sagittal (middle row) and axial view (bottom) of the Colin27 T1-weighted single-subject template brain of the anatomical MNI (Evans et al., 2012) space. Color code indicates percentage of interindividual variability. Red colors indicate low interindividual variability, while blue colors correspond to high variability.

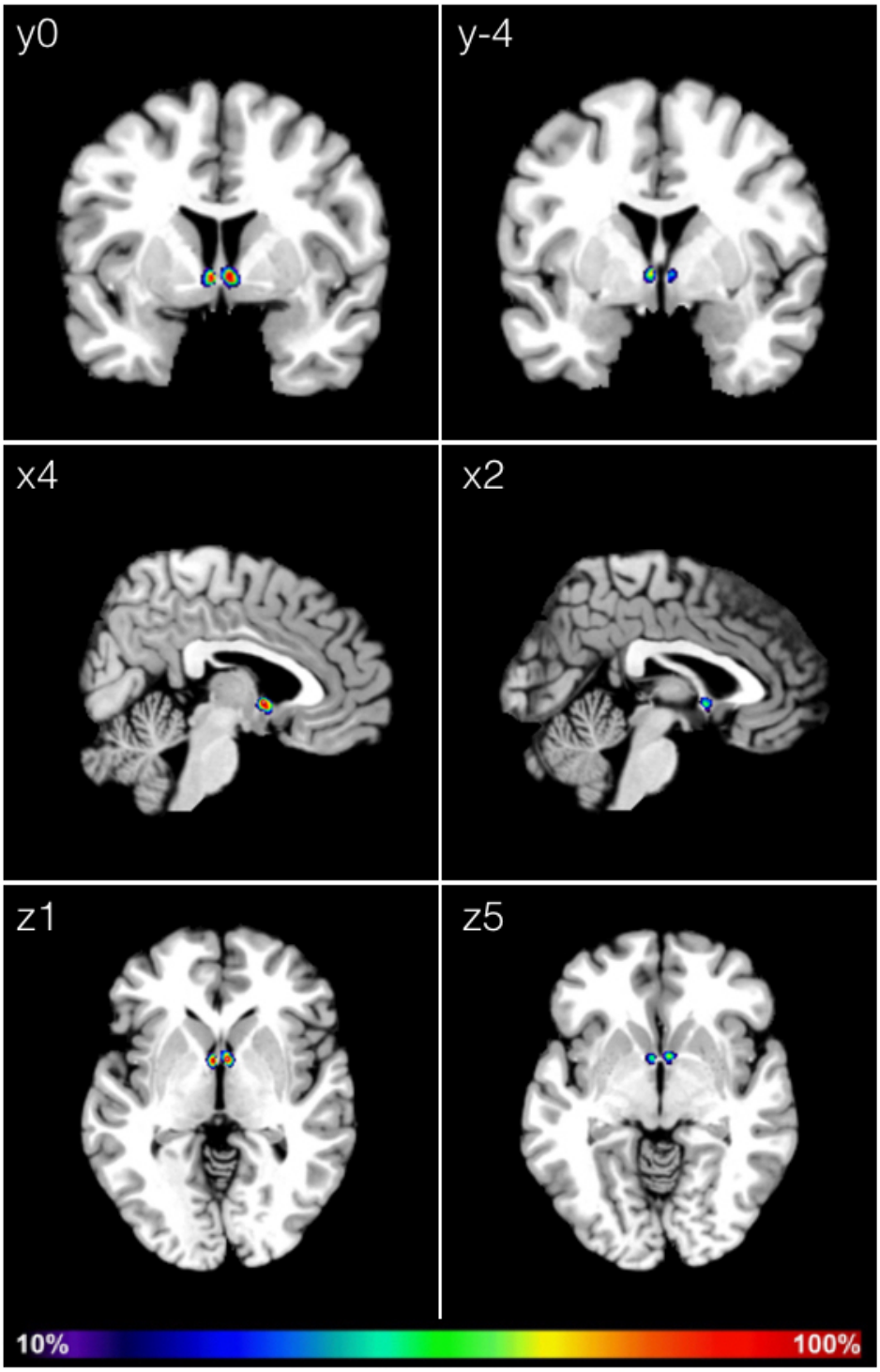

Figure 11: Probabilistic maps of the medial part of the BST in coronal (top), sagittal (middle row) and axial view (bottom) of the Colin27 T1-weighted single-subject template brain of the anatomical MNI (Evans et al., 2012) space. Color code indicates percentage of interindividual variability. Red colors indicate low interindividual variability, while blue colors correspond to high variability.

4 Discussion

In this work the bed nucleus of the stria terminalis was mapped on serial histological sections in ten postmortem brains based on well-accepted cytoarchitectonic criteria (Amunts et al., 1999; Amunts and Zilles, 2015; Brockhaus, 1942). As a result a high-resolution 3D-reconstruction of the bed nucleus was achieved in one individual brain, and probability maps in stereotactic space were created based on mapping in ten brains. While quite detailed studies have been provided in the past for brains of rodents or monkeys (Ju and Swanson, 1989; Martin et al., 1991), this is the first systematic mapping project based on histological sections of human postmortem brains. Results of recent studies, whether it is reasonable to compare findings of rodent model organisms to human results and finally the difficulties of inconsistent nomenclature of the bed nucleus of the stria terminalis (BST) will be discussed in the following.

4.1 Comparison to recent studies

In the past few years the BST has drawn more attention and attempts have been made to describe this small basal forebrain structure stressing out its functional aspects more accurately, also separated from its so far believed co-dependency on the amygdala (Dumont, 2009; Lebow and Chen, 2016). The BST in particular, but not the amygdala, is involved in the circuitry leading information from the hippocampus to the paraventricular nucleus of the hypothalamus and therefore influences the hypothalamic-pituitary-adrenal axis, which is known to be involved in stress response (Lebow and Chen, 2016).
Even studies dealing with the segmentation of the BST have been performed to get an idea of the actual shape and size (Avery et al., 2014; Theiss et al., 2017; Torrisi et al., 2015). The definition of the anterior border of the BST was defined on 3T MRI-scans by 1.8 mm anterior to the decussating anterior commissure and the posterior border was defined by the interventricular foramen (Theiss et al., 2017), which is a good indicator for an average approach but might not consider interindividual differences. Border definitions of such small structures as the BST might be difficult on MR-images due to reduced resolution (1 mm) and contrast of this imaging technique. Border definitions of another study of 7T Magnetic Resonance Imaging (MRI) scans (Avery et al., 2014) were similar defined as by Theiss et al. (2017) by the anterior commissure, the internal capsule and the fornix. Unfortunately, it was not mentioned in these articles, how borders were

defined rostral or caudal from this level.
Volumetric calculations in this work were approximately 10 mm^3 larger than in previous studies (Theiss et al., 2017). These differences could occur due to the fact that also the supracapsular part of the BST was included in the present work, which was not the case in Theiss et al. (2017). The impact of deviating border definitions of these two works could also lead to slight differences in the total volume.
There were no volumetric differences found in the BSTLC between men and women in this work. An earlier paper reported such differences with 39 % larger in males than in females (Chung et al., 2002). However the analysis did not normalize the data, with respect to the overall brain shape. Thus, the reported sexual dimorphism might simply derive from general size differences between both sexes.

4.2 Comparison between primate and non-primate studies

The internal capsule is well-developed and thickened in mammals compared to other vertebrates (Johnston, 1923). This could influence the (small) size of the BST in mammals, which seems to be "squeezed" due to the massive shape of the adjacent internal capsule. However, there are remarkable differences even within mammals, e.g. between rats and humans. Many studies of the bed nucleus of the stria terminalis have been performed on rodents (Alheid et al., 1998; deOlmos and Ingram, 1972; deOlmos and Heimer, 1999; Dong et al., 2001; Ju and Swanson, 1989; McDonald, 1983; Woodhams et al., 1983). Moreover, functional studies in the last years dealing with fear and anxiety, psychiatric disorders or addiction were based on rodent studies (Gungor and Paré, 2016; Lebow and Chen, 2016; Petrovich and Swanson, 1997; Ulrich-Lai and Herman, 2009). As pointed out by Martin et al. (1991), there are indeed similarities according to the compartmentation of the BST, which permits a proper comparison. Additionally, some connections between BST and the CeA known from rodent studies could be confirmed in human studies (Avery et al., 2014).
However, there are important differences between the species. The overall shape of the rodent BST seems to be more short and compact, whereas the human BST has an elongated shape. The BST is better developed in humans than in rodents and seems to have reached its biggest expansion in this species (Andy and Stephan, 1968; Martin et al., 1991). On the contrary, the subcommissural part of the rodent BST seems to be more developed than in the primate one. This might be caused by the fact that the BST is very closely located to the olfactory center, which is better developed in rodents than in humans. Also afferent projections to the BST from the accessory olfactory system, which is involved in pheromone dependent sexual behaviour, have been described (Nieuwenhuys et al., 2008). Although the accessory olfactory system is believed to be absent in adult humans, that is not the case for the influence of pheromones in mating behaviour, so these chemosensory signals might follow other pathways, possibly the terminal nerve connecting the nose with basal forebrain structures (Nieuwenhuys et al., 2008). Hence, even if rats are a common and well-known subject of studies, it should be kept in mind that there are recognizable differences.

Concerning the blood supply of the BST (as described in Chapter 1.1.5), it might be

reasonable to compare rat brains with those of humans, as the main arterial and venous supply resemble similar and same areas in both species. However, the anterior communicating artery, which connects the two anterior cerebral arteries, is very short and less developed in humans than in rats. Medial branches deriving from the anterior communicating artery supply the medial-rostral area of the BST (Danics et al., 1985). Therefore, this supply could be less developed in humans as it was described in rats.

4.3 Inconsistent nomenclature of BST-subdivisions

As mentioned above, the nomenclature of this work mainly follows Heimer et al. (1999) and deOlmos (2004). Differences regarding the partitioning of subdivisions should be noted here. To give an example, Heimer et al. (1999) included the oval subdivision within the laterodorsal part of the BST as its encapsulating thin fiber band. Those two divisions are called central and capsular parts of the dorsolateral bed nucleus. As the delineation in this thesis mostly took place on a resolution of 20 µm, it was not possible to separate the capsular part of the BST due to the slim width of this band and therefore it was not possible to include it in the mapping. The central part was further traced separately from the BSTLD, but can be considered as a subdivision of the BSTLD. However, other authors state, that the BSTLC is on the same hierarchical level as the BSTLD and BSTM (Lesur et al., 1989; Mai et al., 2007). In any case the oval subdivision plays a distinct role and is involved in several functional processes. Its putative sexual dimorphism was already discussed in Chapter 4.1.
According to some authors, there is a subdivision called the juxtacapsular BST, which is part of the BSTL (Heimer et al., 1999; deOlmos, 2004). It is situated on the lateral side of the BSTLD, between the BSTLC and the internal capsule. During the mapping this subdivision was visible on several sections. Still, it was not compartmented, but included in the subdivision of the BSTLD, as it was only detectable on very few sections and the distinction to other subdivisions was not clearly defined.
The lateroventral part, which Heimer et al. (1999) abbreviated as BSTLV, was considered to be the subdivision found ventral to the anterior commissure. Images contained only subdivisions, where the commissure was decussating and therefore these two subdivisions were clearly to separate. How the distinction between BSTLD and BSTLV on levels shortly after the crossing, was not shown or described. For this reason and the fact that it was cytoarchitectonically not possible to distinguish between these two areas dorsal and ventral of the commissure, it was decided that there is only one subdivision, called BSTLD. Furthermore, this ventral part of the BST was not found in every brain and throughout all sections of the crossing of the commissure. Furthermore, this nomenclature might derive from non-primate literature, as this area seems to be quite evolved in rodents.
Moreover, it seems that interface islands tend to cluster alongside the anterior commissure and at its lateral ends and therefore might be mistaken as part of the BST, which contains very similar islets. However, these granular, very densely packed cell aggregates contain even smaller neurons than interface islands of the BST. Such islands appear frequently in the sublenticular part of the BST, which were not considered as part of the BST by deOlmos (2004)

Another difference between our nomenclature and the differentiation of the BST used by Heimer et al. (1999) is the separation of the medial subdivision in an anterior and posterior part. These can be even further subdivided into dorsolateral and ventromedial part of the anterior BSTM and the posterior could be parted into three more subdivisions. It was decided not to make any further subdivisions here, as the BSTM is a very small structure and due to its heterogeneous appearance, which makes a differentiation from other adjacent structures impossible, at least on the level of cytoarchitectonic criteria.

5 Outlook: Approaches of multimodality

Cytoarchitecture represents one important aspect of brain organisation. However, other modalities are also important to get a comprehensive understanding of the organisational principles of the bed nucleus. To address such apsects, two different methods were employed as a pilot study, to get prospective ideas, to examine the bed nucleus of the stria terminalis in more detail in the future.
Quantitative receptorautoradiography is a method to analyze the molecular architecture of the brain, based on the distribution of receptors of neurotransmitters and to detect borders based on different receptor densities in various brain areas. Secondly, fiber architecture reveals information about structural link between brain regions. These two methods will be briefly introduced and discussed.

5.1 Receptorautoradiography

Receptorautoradiographic method is an approach based on the analysis of densities of neurotransmitter receptors. Cryofixed brain tissue was serially sectioned. Alternating sets of sections were opposed to [^{3}H]-radioactively labeled receptor-ligands of six different transmitter systems (i.e. serotoninergic, dopaminergic, GABAergic, glutamatergic, adrenergic and cholinergic). After incubation the sections were exposed to a β-sensitive film for several weeks, resulting in grey values and the absolute concentrations of receptors in femtomol per milligram protein. Images were digitized and pseudocolored. For detailed description of this method, refer to Zilles et al. (2002). Receptor autoradiograms sometimes reveal a very fine-grained parcellation of a brain structure, which was the reason to apply this method with respect to the BST using the cholinergic muscarinic M_3 receptor.

Borders on the histological image (Fig. 12 a) were drawn based on the applied cytoarchitectonic criteria, as described in Chapter 3.1 in neighboring sections in which the different receptor types have been revealed. The ligand of the example shown in Figure 12 (b) is 4-DAMP, an antagonist of the muscarinic acetylcholine M_3 receptor. Slight differences between both images are given as both images are not directly adjacent to each

other (distance approximately 100 µm) and the BST is a very small structure, changing its shape quite rapidly. Nevertheless all four subdivisions and the main shape of this BST of the right hemisphere can be recognized on both images. The BSTLC contains higher densities of this receptor than its surrounding BSTLD and the adjacent BSTM. The subdivision with least receptor densities per mg protein is BSTLP, indicated by light and dark blue colors (Fig. 12 b). The BSTLC is separated into two parts at this level. Its two parts still can be associated with each other due to the similar amount of receptor densities, which is also in accordance to cytoarchitectonic findings. The two interface islands, marked by asterisks, have higher densities of receptors than the BSTLC and are therefore clearly distinguished from this subdivision. Therefore, the clear distinction made already due to cytoarchitectonic findings between BSTLC and interface islands can be confirmed also by receptorautoradiography.
This method has also been used in the past for subcortical areas (Graebenitz et al., 2011; Zaborszky et al., 2008) and should therefore be pursued in future studies of the BST.

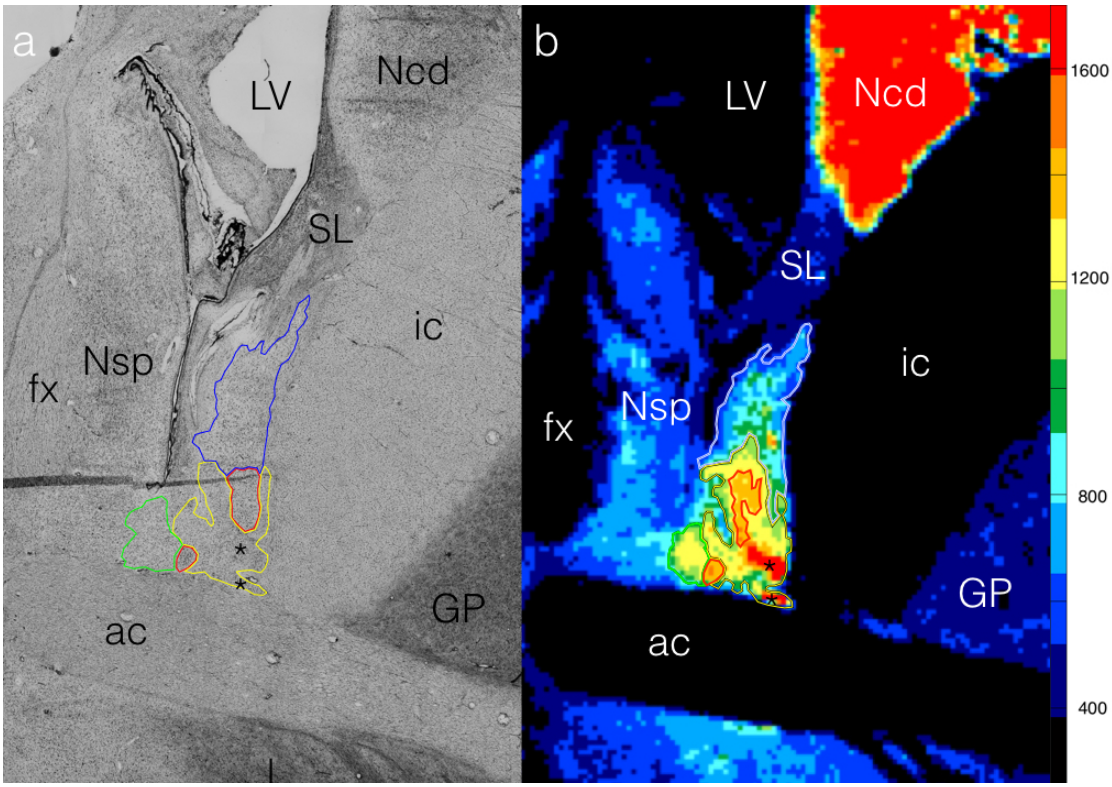

Figure 12: Cell-body stained histological section (a) and receptorautoradiography (b) of a right hemisphere bed nucleus. Red: BSTLC, yellow: BSTLD, blue: BSTLP and green: BSTM. (b) Densities of the muscarinic acetylcholin M_3-receptor (4-DAMP) in a coronal section. Receptor densities in fmol/mg protein as indicated in the scale on the right side. Subdivision with highest levels of 4-DAMP is BSTLC. BSTLD and BSTM have intermediate levels of receptor densities and BSTLP has least. The asterisks mark interface islands in both images, containing very high levels of 4-DAMP. Abbreviations: ac - anterior commissure, fx - fornix, GP - Globus pallidus, ic - internal capsule, LV - lateral ventricle, Ncd - nucleus caudatus, Nsp - Nucleus septalis, SL - subependymal layer.

5.2 Polarized Light Imaging

Three-dimensional Polarized Light Imaging (PLI) is an optical technique to analyze spatial orientation and architecture of nerve fibers based on the birefringence of myelin as measured by a polarimeter (Axer et al., 2011). The techniques used for image acquisition and data processing down to the fiber orientation maps were previously described in detail by Axer et al. (2011). The detection of fiber pathways is a complementary method for cytoarchitectonical analysis in order to gain information about fiber connections.

The architecture of nerve fibers can be visualized using HSV-colormaps encoding their spatial orientation by colors. The hue (H) value of a pixel represents the prevailing in-plane direction of the fibers in the corresponding voxel while the saturation (S) and the intensity value (V) represent their out-of-plane inclination. A typical HSV-color code for PLI-Fiber orientation maps is shown in the upper right corner of Figure 13. The dark areas represent steep fibers, the colored areas near the equator more flat fibers.

Figure 13 shows the BST and its surrounding structures. Pink and red colors indicate almost horizontal fibers, whereas green and blue colors represent vertical running fibers. The latter can be observed at the BST, which contains predominantly fibers in vertical directions. It can be inferred that the encapsulated, oval-shaped subdivision of the bed nucleus, i.e. BSTLC, is also visible here, as marked by the dashed line. There are connections linking caudate nucleus and BST, and between septal nuclei and BST as well. On the contrary, the sharp border between the BST and the internal capsule indicates that there are almost no connections between those structures at this level of coronal section planes.

Thus, 3D-PLI seems to be capable to address the complex fiber architecture of the human brain in this particular region. Our preliminary data seem to agree with earlier findings that there are indeed links between the BST and limbic or thalamic structures as well as basal ganglia, such as the caudate nucleus. Missing connections to the internal capsule recently suggested by Krüger et al. (2015), seems likely to be confirmed also by PLI. To approach this question in more detail, a systematic analysis of the bed nucleus would be mandatory.

5.3 Conclusion

In summary, the four subdivisions, as parts of the two subnuclei of the bed nucleus, were identified on the basis of cytoarchitectonic mapping. The mapping resulted in the generation of high-resolution 3D-reconstruction and probabilistic maps, which are the first of its kind for the human brain. Probabilistic maps in stereotactic space consider intersubject variability of the lateral and medial subnuclei of the bed nucleus. They can be used as an anatomical reference for the interpretation of various imaging data, such as functional MRI or Positron Emission Tomography (PET), of healthy subjects or patients. In addition, the mapping provides a good basis for other modalities, as receptorautoradiography on a molecular level or Polarized Light Imaging to visualize

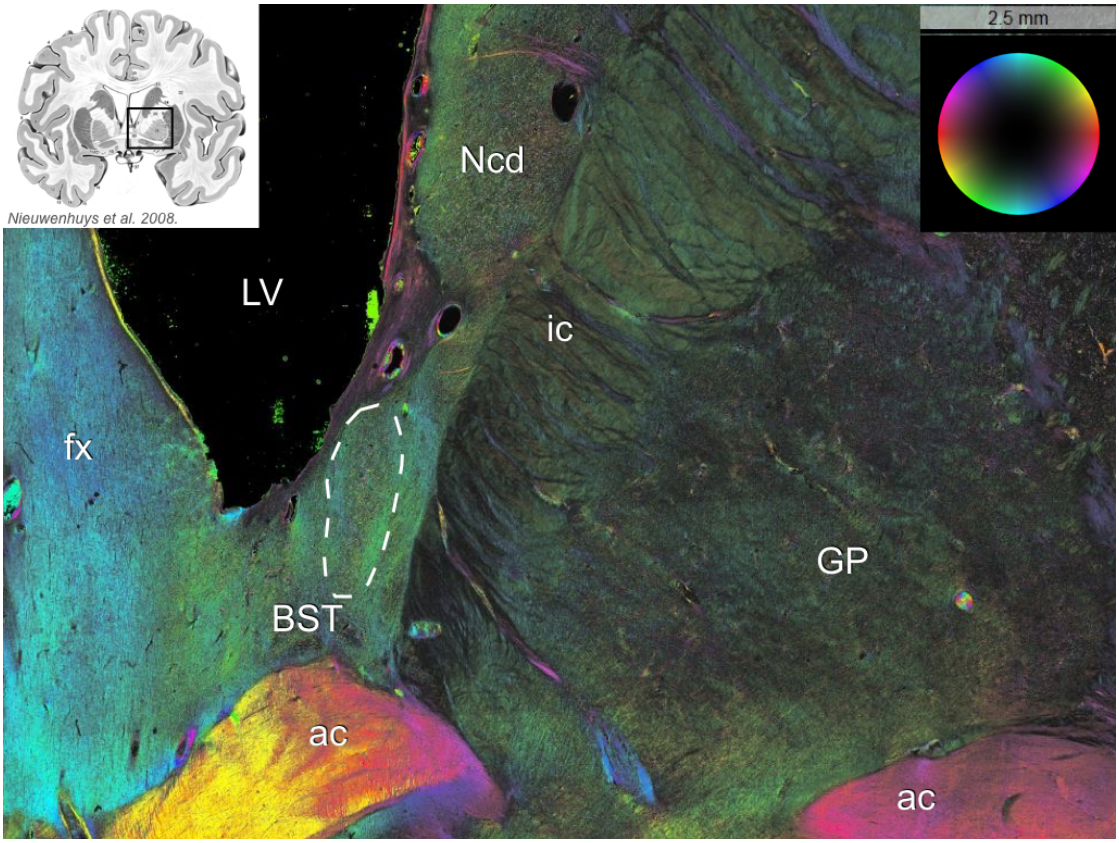

Figure 13: 3D-Polarized Light Imaging revealing fiber architecture of the BST. Fiber directions can be derived by the color code on the top right corner. Note that there seem to be strong connections between BST and caudate nucleus, indicated by similar colors. Almost no connections between BST and internal capsule or the anterior commissure are visible in this sectioning plane. The laterocentral subdivision of the bed nucleus (BSTLC) is delineated by a dashed line. Abbreviations: ac - anterior commissure, BST - bed nucleus of the stria terminalis, fx - fornix, GP - Globus pallidus, ic - internal capsule, LV - lateral ventricle, Ncd - caudate nucleus.

fiber architecture, by giving additional information of the bed nucleus. Further studies are necessary for a better understanding of this particular region.

Bibliography

Alheid, G. F., C. A. Beltramino, J. S. deOlmos, M. S. Forbes, D. J. Swanson, and L. Heimer (1998). The neuronal organization of the supracapsular part of stria terminalis in the rat: the dorsal component of the extended amygdala. *Neuroscience 84*(4), 967–996.

Amir, S. and J. Stewart (2009). Behavioral and hormonal regulation of expression of the clock protein, PER2, in the central extended amygdala. *Progress in Neuro-Psychopharmacology and Biological Psychiatry 33*(8), 1321–1328.

Amunts, K., O. Kedo, M. Kindler, P. Pieperhoff, H. Mohlberg, N. J. Shah, U. Habel, F. Schneider, and K. Zilles (2005). Cytoarchitectonic mapping of the human amygdala, hippocampal region and entorhinal cortex: intersubject variability and probability maps. *Anatomy and Embryology 210*(5-6), 343–352.

Amunts, K., C. Lepage, L. Borgeat, H. Mohlberg, T. Dickscheid, M.-E. Rousseau, S. Bludau, P.-L. Bazin, L. B. Lewis, A.-M. Oros-Peusquens, N. J. Shah, T. Lippert, K. Zilles, and A. C. Evans (2013). BigBrain: An Ultrahigh-Resolution 3D Human Brain Model. *Science 340*, 1472–1475.

Amunts, K., A. Schleicher, U. Bürgel, H. Mohlberg, H. B. M. Uylings, and K. Zilles (1999). Broca's Region Revisited: Cytoarchitecture and Intersubject Variability. *Journal of Comparative Neurology 412*, 319–341.

Amunts, K., A. Schleicher, and K. Zilles (2007). Cytoarchitecture of the cerebral cortex–more than localization. *NeuroImage 37*(4), 1061–1065.

Amunts, K. and K. Zilles (2015). Architectonic mapping of the human brain beyond brodmann. *Neuron 88*(6), 1086–1107.

Andy, O. J. and H. Stephan (1968). The Septum in the Human Brain. *Journal of Comparative Neurology 133*, 383–410.

Avery, S. N., J. A. Clauss, and J. U. Blackford (2016). The Human BNST: Functional Role in Anxiety and Addiction. *Neuropsychopharmacology 41*(1), 126–141.

Avery, S. N., J. A. Clauss, D. G. Winder, N. Woodward, S. Heckers, and J. U. Blackford (2014). BNST neurocircuitry in humans. *NeuroImage 91*, 311–323.

Axer, M., K. Amunts, D. Grässel, C. Palm, J. Dammers, H. Axer, U. Pietrzyk, and K. Zilles (2011). A novel approach to the human connectome: Ultra-high resolution mapping of fiber tracts in the brain. *NeuroImage 54*(2), 1091–1101.

Baroncini, M., P. Jissendi, E. Balland, P. Besson, J. P. Pruvo, J. P. Francke, D. Dewailly, S. Blond, and V. Prevot (2012). MRI atlas of the human hypothalamus. *NeuroImage 59*(1), 168–180.

Bludau, S., S. B. Eickhoff, H. Mohlberg, S. Caspers, A. R. Laird, P. T. Fox, A. Schleicher, K. Zilles, and K. Amunts (2014). Cytoarchitecture, probability maps and functions of the human frontal pole. *NeuroImage 93 Pt 2*, 260–275.

Brockhaus, H. (1942). Zur feineren Anatomie des Septum und des Striatum. *Journal für Psychologie und Neurologie 51*, 1–56.

Chung, W. C. J., G. J. deVries, and D. F. Swaab (2002). Sexual Differentiation of the Bed Nucleus of the Stria Terminalis in Humans May Extend into Adulthood. *Journal of Neuroscience 22*(3), 1027–1033.

Dabrowska, J., D. Martinon, M. Moaddab, and D. G. Rainnie (2016). Targeting corticotropin-releasing factor (CRF) projections from the oval nucleus of the BNST using cell-type specific neuronal tracing studies in mouse and rat brain. *Journal of Neuroendocrinology 28*(12), 1–15.

Danics, Z., S. Horváth, and M. Palkovits (1985). Blood supply of the bed nucleus of the stria terminalis in rat. *Cell and Tissue Research 241*, 445–451.

Davis, M., D. L. Walker, L. Miles, and C. Grillon (2010). Phasic vs sustained fear in rats and humans: role of the extended amygdala in fear vs anxiety. *Neuropsychopharmacology 35*(1), 105–135.

deOlmos, J. (2004). Amygdala. In G. Paxinos and J. Mai (Eds.), *The Human Nervous System* (2nd ed.)., Chapter 22, pp. 739–868. San Diego, California, USA: Elsevier Academic Press.

deOlmos, J. S. and L. Heimer (1999). The Concepts of the Ventral Striatopallidal System and Extended Amygdala. *Annals of the New York Academy of Sciences 29*(877), 1–32.

deOlmos, J. S. and W. Ingram (1972). The Projection Field of the Stria Terminalis in the Rat Brain An Experimental Study. *Journal of Comparative Neurology 146*(3), 303–334.

Di Marino, V., M. Niddam, and Y. Etienne (2016). The Bed Nucleus of the Stria Terminalis. In V. Di Marino (Ed.), *The amygdaloid nuclear complex*, Chapter 10, pp. 111–119. Springer.

Dong, H. W., G. D. Petrovich, and L. W. Swanson (2001). Topography of projections from amygdala to bed nuclei of the stria terminalis. *Brain Research Reviews 38*, 192–246.

Dumont, E. C. (2009). What is the bed nucleus of the stria terminalis? *Progress in Neuropsychopharmacology and Biological Psychiatry 33*(8), 1289–1290.

Evans, A., A. Janke, D. Collins, and B. S. (2012). Brain templates and atlases. *NeuroImage 62*(2), 911–922.

Evans, A., S. Marrett, P. Neelin, L. Collins, K. Worsley, W. Dai, S. Milot, E. Meyer, and D. Bub (1992). Anatomical mapping of functional activation in stereotactic coordinate space. *NeuroImage 1*, 43–53.

Fudge, J. L. and S. N. Haber (2001). Bed nucleus of the stria terminalis and extended amygdala inputs to dopamine subpopulations in primates. *Neuroscience 104*(3), 807–827.

Graebenitz, S., O. Kedo, E.-J. Speckmann, A. Gorji, H. Panneck, V. Hans, N. Palomero-Gallagher, A. Schleicher, K. Zilles, and H.-C. Pape (2011). Interictal-like network activity and receptor expression in the epileptic human lateral amygdala. *Brain 134*(10), 2929–2947.

Gungor, N. Z. and D. Paré (2016). Functional Heterogeneity in the Bed Nucleus of the Stria Terminalis. *Journal of Neuroscience 36*(31), 8038–8049.

Heimer, L., J. S. deOlmos, G. F. Alheid, J. Pearson, N. Sakamoto, K. Shinoda, J. Marksteiner, and R. C. Switzer (1999). The human basal forebrain, Part II. In F. E. Bloom, A. Björklund, and T. Hökfeld (Eds.), *Handbook of chemical Neuroanatomy*, Volume 15 of *The Primate Nervous System*, Chapter 2, pp. 57–226. Amsterdam: Elsevier.

Heimer, L. and G. W. van Hoesen (2006). The limbic lobe and its output channels: implications for emotional functions and adaptive behavior. *Neuroscience and Biobehavioral Reviews 30*(2), 126–147.

Holstege, G., L. Meiners, and K. Tan (1985). Projections of the bed nucleus of the stria terminalis to the mesencephalon, pons, and medulla oblongata in the cat. *Experimental Brain Research 58*, 379–391.

Johnston, J. B. (1923). Further Contributions to the Study of the Evolution of the Forebrain. *Journal of Comparative Neurology 35*(5), 337–481.

Ju, G. and L. W. Swanson (1989). Studies on the Cellular Architecture of the Bed Nuclei of the Stria Terminalis in the Rat: I. Cytoarchitecture. *The Journal of Comparative Neurology 280*, 587–602.

Kim, S.-Y., A. Adhikari, S. Lee, J. Marshel, C. Kim, C. Mallory, M. Lo, S. Pak, J. Mattis, B. Lim, M. R.C., M. Warden, R. Neve, K. Tye, and K. Deisseroth (2013). Diverging neural pathways assemble a behavioural state from separable features in anxiety. *Nature 496*, 219–223.

Krüger, O., T. Shiozawa, B. Kreifelts, K. Scheffler, and T. Ethofer (2015). Three distinct fiber pathways of the bed nucleus of the stria terminalis to the amygdala and prefrontal cortex. *Cortex 66*, 60–68.

Lebow, M. A. and A. Chen (2016). Overshadowed by the amygdala: the bed nucleus of the stria terminalis emerges as key to psychiatric disorders. *Molecular Psychiatry 21*(4), 450–463.

Lesur, A., P. Gaspar, C. Alvarez, and B. Berger (1989). Chemoanatomic compartments in the human bed nucleus of the stria terminalis. *Neuroscience 32*(1), 181–194.

Mai, J. K., G. Paxinos, and T. Voss (2007). Atlas of the human brain in stereotaxic coordinates. In *Atlas of the Human Brain* (3rd ed.). San Diego: Elsevier Academic Press.

Martin, L. J., R. E. Powers, T. L. Dellovade, and D. L. Price (1991). The Bed Nucleus-Amygdala Continuum in Human and Monkey. *Journal of Comparative Neurology 309*, 445–485.

McDonald, A., S. Shammah-Lagnado, C. Shi, and M. Davis (1999). Cortical Afferents to the Extended Amygdala. *Annals of the New York Academy of Sciences 877*, 309–338.

McDonald, A. J. (1983). Neurons of the Bed Nucleus of the Stria Terminalis: A Golgi Study in the Rat. *Brain Research Bulletin 10*, 111–120.

Merker, B. (1983). Silver staining of cell bodies by means of physical development. *Journal of Neuroscience Methods 9*, 235–241.

Mohlberg, H., B. Tweddell, T. Lippert, and K. Amunts (2016). Workflows for Ultra-High Resolution 3D Models of the Human Brain on Massively Parallel Supercomputers. In K. Amunts, L. Grandinetti, T. Lippert, and N. Petkov (Eds.), *Brain-Inspired Computing, Second International Workshop*, pp. 15–27. Heidelberg: Springer.

Nieuwenhuys, R., J. Voogd, and C. van Huijzen (2008). Telencephalon: Amygdala and claustrum. In R. Nieuwenhuys, J. Voogd, and C. van Huijzen (Eds.), *The Human Central Nervous System* (4th ed.)., Chapter 13, pp. 401–426. Berlin Heidelberg New York: Springer.

Petrovich, G. and L. Swanson (1997). Projections from the lateral part of the central amygdalar nucleus to the postulated fear conditioning circuit. *Brain Research 763*(2), 247–254.

Sanides, F. (1957). Die Insulae terminales des Erwachsenengehirns des Menschen. *Journal für Hirnforschung 3*(2), 243–273.

Somerville, L. H., P. J. Whalen, and W. M. Kelley (2010). Human bed nucleus of the stria terminalis indexes hypervigilant threat monitoring. *Biological Psychiatry 68*(5), 416–424.

Theiss, J. D., C. Ridgewell, M. McHugo, S. Heckers, and J. U. Blackford (2017). Manual segmentation of the human bed nucleus of the stria terminalis using 3T MRI. *NeuroImage 146*, 288–292.

Torrisi, S., K. O'Connell, A. Davis, R. Reynolds, N. Balderston, J. Fudge, C. Grillon, and M. Ernst (2015). Resting state connectivity of the bed nucleus of the stria terminalis at ultra-high field. *Human Brain Mapping 36*, 4076–4088.

Ulrich-Lai, Y. M. and J. P. Herman (2009). Neural regulation of endocrine and autonomic stress responses. *Nature Reviews Neuroscience 10*(6), 397–409.

Walter, A., J. K. Mai, L. Lanta, and T. Görcs (1991). Differential Distribution of Immunohistochemical Markers in the Bed Nucleus of the Stria Terminalis in the Human Brain. *Journal of Chemical Neuroanatomy 4*, 281–298.

Woodhams, P. L., G. W. Roberts, J. M. Polak, and T. J. Crow (1983). Distribution of neuropeptides in the limbic system of the rat: the bed nucleus of the stria terminalis, septum and preoptic area. *Neuroscience 8*(4), 677–703.

Yassa, M. A., R. L. Hazlett, C. E. L. Stark, and R. Hoehn-Saric (2012). Functional MRI of the amygdala and bed nucleus of the stria terminalis during conditions of uncertainty in generalized anxiety disorder. *Journal of Psychiatric Research* (8), 1045–1052.

Zaborszky, L., L. Hoemke, H. Mohlberg, A. Schleicher, K. Amunts, and K. Zilles (2008). Stereotaxic probabilistic maps of the magnocellular cell groups in human basal forebrain. *NeuroImage 42*(3), 1127–1141.

Zilles, K., A. Schleicher, N. Palomero-Gallagher, and K. Amunts (2002). Quantitative Analysis of Cyto- and Receptor Architecture of the Human Brain. In A. W. Toga and J. C. Mazziotta (Eds.), *Brian Mapping: The Methods*, Chapter 21, pp. 573–602. Amsterdam: Elsevier.